Highlights from Beam Diagnostics

H. Schmickler,
CERN, Geneva, Switzerland

Abstract

The quality of beam diagnostics is very important in accelerators for the optimization of machine paerformance and for the understanding of accelerator physics issues. Many examples of successful and outstanding beam instrumentation at different accelerators will be shown highlighting the following aspects:

- ultimate measurement resolution in space and time obtained exploiting different detection principles
- clever use of standard instrumentation tools
- benefit for beam instrumentation obtained from introducing digital signal treatment techniques.

1 GENERAL ASPECTS

When preparing this presentation I often asked myself the question of the definition of a "highlight" of beam instrumentation.

Naturally one would consider instruments with exceptional time or space resolution as a potential highlight. Such new developments based on the exploitation of new physics principles have been demanded for new accelerators and are the result of many man years of development. As examples of this type of highlights I will describe the two detectors successfully tested at the final focus test beam facility at SLAC for submicron beam size measurements and two detectors for measuring the length of picosecond or subpicosecond bunches.

But there must be more highlights in beam instrumentation! And indeed one should look at the work that has been done with instruments that have been designed for ordinary daily use in any control room. And there one finds clever measurement procedures making use of these instruments in a different way and hence giving insights to undiscovered phenomena. Several examples of this type will be reported.

Last not least some beam instrumentaion highlights are based on the ever increasing amount of available computing power. Online displays in control rooms or real time feedbacks which were impossible to realize ten years ago have become possible now. This development will also be demonstrated by a few examples.

2 SOPHISTICATED DETECTORS

For this paragraph in total four examples have been selected, the first two focusing on detectors for ultimate space resolution at the Slac Final Focus Test Beam Facility, where beam sizes below 100 nm have to be measured.

The other two examples present detectors for bunch length measurements in the picosecond and subpicosecond domain, both detectors based on autocorrelation techniques. From CERN for the LEP storage ring a single shot optoelectronic autocorrelation circuit and from SLAC for the SUNSHINE facility a pure optical autocorrelation device.

In all cases only the basic idea of the detector will be described. For more details one has to consult the references.

2.1 Submicronic Beam Size Monitors at SLAC FFTB

- **Nanometer Spot Size Monitor using Laser Interferometery [1]**

The basic idea of this detector is illustrated in figure 1. The beam is steered across a grid and the interaction of the beam with the grid is measured. As the beam sizes σ_y are of the order of 100 nm any mechanical grid is excluded.

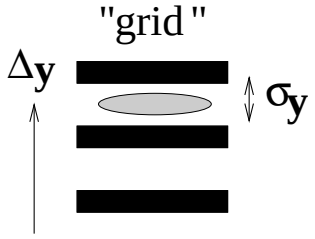

Figure 1: Schematic drawing of the measurement principle.

The remarkable achievement of the collaboration [1] is to use the interference fringe of two laser beams as interaction "grid". The complete detector setup is shown in figure 2. The interaction of the beam with the photons from the laser is measured by counting compton scattered photons downstream of the interaction region. As the laser is runing at a repetition rate of 10 Hz but the beam is produced at 30 Hz rate, the actual photon counting rate is the difference between two dark current measurements and one aquisition with the laser beams present. Figure 3 gives a measurement example. The final measurement quantity, the beam size σ_y, has to be extracted from the measurements as illustrated in figure 4. The observable signal is the modulation depth $M = \frac{B}{A}$. M is extracted from the data by a fit and the beam size σ_y is calculated from the indicated formula. For the data

shown in figure 4 one obtains $\sigma_y = 66 \pm 3$ nm. More details on this detector can be found in [1]

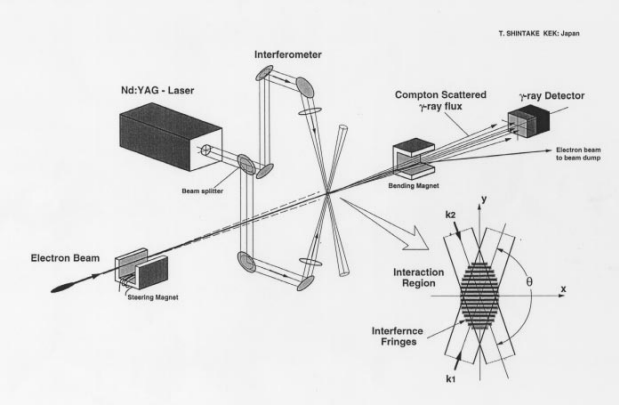

Figure 2: Detector layout

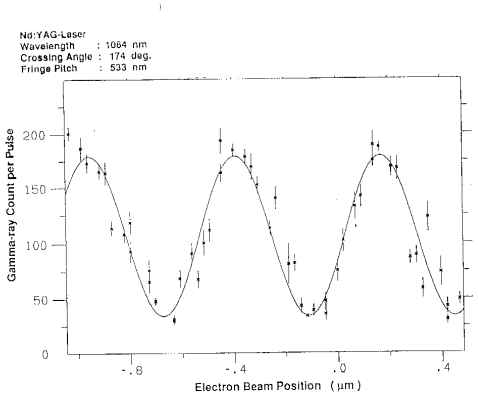

Figure 3: Measurement example

$$M = \frac{B}{A} \sim e^{-2k_y^2 \cdot \sigma_y^{*2}}$$

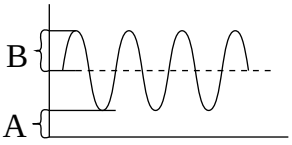

Figure 4: Evaluation of σ_y

• Gas-Ionization beam size Monitor [2]

This detector is installed next to the detector described above. It is based on a completely different detection principle. Here the general idea is to make the electron beam interact with gas ions (He^+ ions) and to observe those gas ions which have been accelerated transversely by the space charge fields of the passing electron beam. Figure 5 shows the detector layout. One can see the gas inlet and the micro channel plates for the ion detection surrounding the interaction region.

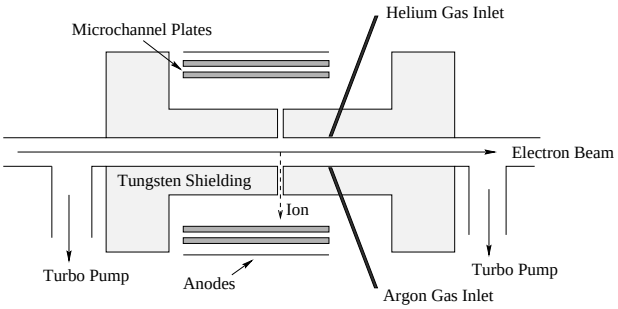

Figure 5: Detector layout

With the nominal parameters of the FFTB, i.e. beam sizes of $1.8\mu m \cdot 60nm$ space charge fields of 800 MV/m are produced and the accelerated He^+ ions will reach up to 10 keV energy. The velocity of the ions is proportional to their energy, which in turn is inversely proportional to the horizontal beam size of the passing electrons (approximation for flat beams). The velocity is inversely proportional to the observable parameter, which is the time of flight of the arriving He^+ ions. Hence we can write:

$$1/T_{min} \simeq \beta_{max} \simeq E_{max} \simeq 1/\sigma_x \qquad (1)$$

Figure 6 shows a measurement example for the time of flight distribution. These distributions can be used in a range from $\sigma_x = 70\mu m$ corresponding to ion energies below 10 eV down to $\sigma_x = 2\mu m$ corresponding to ion energies of about 10 keV.

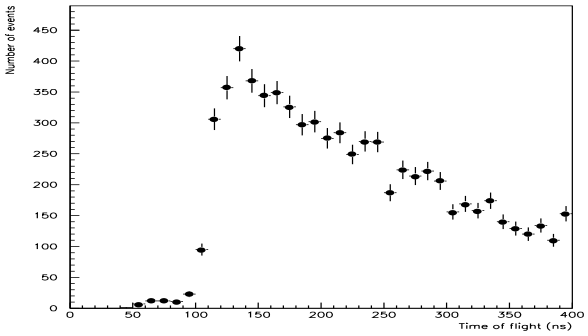

Figure 6: Measurement example of the time of flight distribution of the He^+-ions.

For the FFTB the vertical dimension of the beams is of larger importance. This quantity can be obtained from the azimutal distribution of the He^+ ions. During the passage of the electron beam there is enough time for the ions to oscillate in the potential well of the passing beam. Due to this oscillation the ions are emitted azimutally according to the shape of the potential well. This well is symmetric for round beams, i.e. in this case the azimutal distribution of the detected ions would be isotropic. In case of a flat beam the ions are emitted predominately to the sides creating two peaks at 180^0 angular distance in the azimutal distribution. One can show that from the A2-Fourier Coefficient of this distribution one can determine the vertical dimension σ_y of the

beams. Figure 7 shows a measurement example. Useful information can be obtained for the range σ_y = 500 nm down to σ_y = 70 nm. For more details one has to refer to [2].

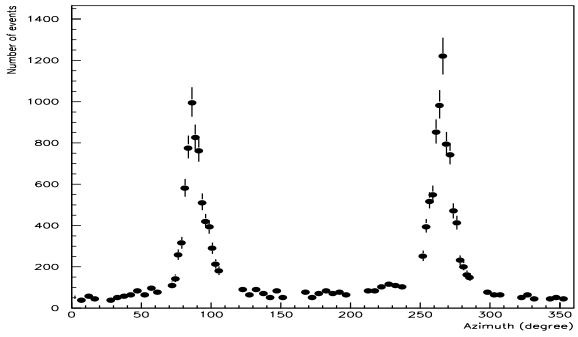

Figure 7: Measurement example of the azimutal distribution of the He^+-ions.

2.2 *Single Shot bunch length measurements at LEP (Autocorrelator)*

Having treated two detectors with ultimate space resolution I shall cover now two examples of detectors for bunch length measurements in the picosecond and subpicosecond domain. For this time resolution electronic devices are too slow, hence one has to exploit at least optoelectronic components where rise times of 300 fsec have been reached [4].

Based on Cd-Te photoconductors an optoelectronic sampler for the LEP bunches has been constructed [3]. Figure 8 shows the layout of the detector. Several Cd-Te photoconductors are simultaneously exposed to the X-ray part of the synchrotron radiation of the LEP lepton bunches. The central photoconductor is polarized by a large DC-voltage. On arrival of the X-rays the central photoconductor emits an electric signal into a matched delay line connected to the other photoconductors.

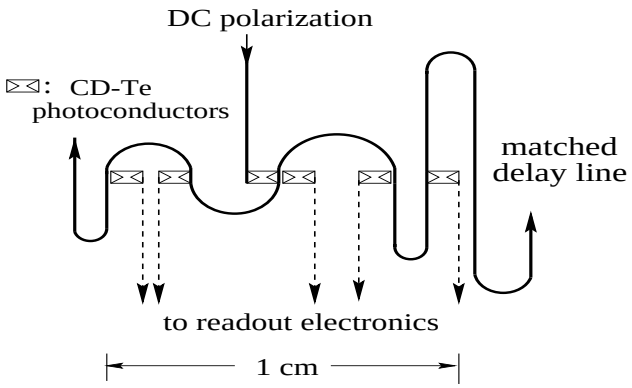

Figure 8: Detector schema of an optoelectronic sampler (autocorrelation principle) for LEP bunches.

These photoconductors will be polarized now by this electrical pulse, which represents the time distribution of the x-rays and hence the longitudinal profile of the leptons. As all photoconductors are exposed to the same x-ray pulse the autocorrelation signal traveling to the integrators in the readout electronics give a signal depending on the bunch length and the electric delay on the circuit. Using all signals from the photocunductors the longitudinal distribution of the leptons can be reconstructed. The delays between photoconductors has been chosen to cover several sigma of the nominal 40 psec bunch length of LEP. The detector will be installed in the LEP tunnel in october 1996, as measurement result figure 9 shows data obtained from a test run.

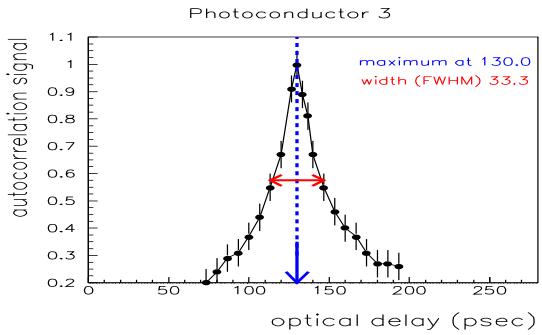

Figure 9: Test data for one of the photoconductors of the circuit shown in figure 8

During this test run the autocorrelator was exposed to the light of a laser with a FWHM pulse lenght below 10 psec. The laser light was split and the central photoconductor was directly exposed to the laser light, whereas each other photoconductor was exposed via an optical delay. If the optical delay matches the electrical delay of the delay line the autocorrelation signal must be maximum. These tests have shown that the detector works and from the width of the distribution (figure 9) one can deduce the time resolution of the optoelectronic elements.

2.3 *Measurement of 50-fs (rms) Electron Pulses*

This detector [5] has been developed for the SUNSHINE facility at SLAC, where electron bunches short as 50 fs (rms) can be produced and measured. This presentation is a nice occasion to mention that for this work W. Berry and H. Lihn, have been awarded the "**Faraday Cup Award 1996**", an award honoring innovative beam instrumentation.

As the LEP detector the device is based on autocorrelation techniques. For the time resolution in question even optoelectronic devices are too slow, hence the autocorrelation is obtained by pure optical means. More precisely a Michelson interferometer is used to split the beam signal and to create the optical delay. Figure 10 gives details of the experimental setup and figure 11 gives a measurement example. The measured width of 24μm translates into 120 fs bunchlength in case the shape was gaussian or 160 fs for a rectangular longitudinal distribution.

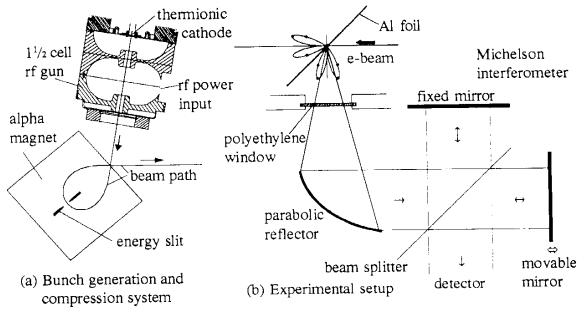

Figure 10: Schematic diagrams of (a) the bunch generation and compression system used at SUNSHINE and (b) the experimental setup.

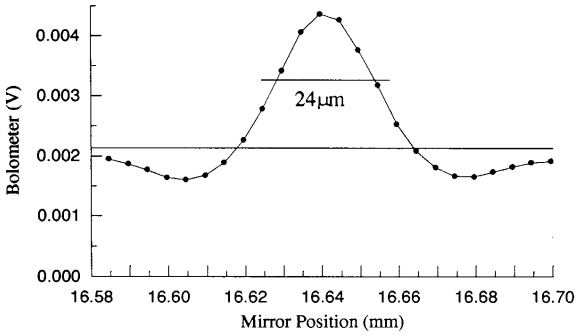

Figure 11: Fine autocorrelation scan of the main peak for the shortest electron bunch length obtained at SUNHINE.

3 CLEVER MEASUREMENT PROCEDURES

3.1 Central Frequency of LEP

This type of measurement has already been done at DESY and other machines and it has been proposed for LEP by A. Hofmann. The aim is to define the geometrical center of the machine with a measurement procedure. One exploits ordinary chromaticity measurements, for which the variation of the betatron tunes is measured as a function of the beam energy, i.e. as a function of the Rf-frequency. If one repeats the chromaticity measurements for several chromaticity settings one obtains results as show in figure 12.

All chromaticity measurements cross in one point. This is obviously the point where the beam passes through the center of the sextupoles as the betatron tune is independent of the powering of the sextupoles. In most machines the sextupoles are fixed together with the quadrupoles on one girder. Therefore the center of the sextupoles is a good definition of the center of the machine.

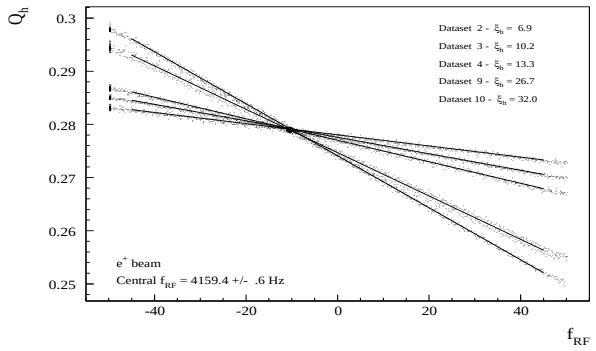

Figure 12: Measurement example of the central frequency of LEP.

One might have the impression that the above measurement is very academic. But over a period of weeks central frequency measurements have been made at LEP in 1993 [6]. The observed variation in the LEP central frequency is nicely correlated with the change of the LEP beam energy due to tidal effects [7]. The above measurements have confirmed the assumption that tidal forces vary the energy of the LEP beams at the 10^{-5} level by changing the circumference (and hence the central frequency) of the machine.

3.2 Beam Based Pickup Calibration at LEP

Similar to the previous example this method is based on the detection of the beam passage through the center of a magnetic element. If one takes a single quadrupole and one could detect by same means that the beam passes through its magnetic center the reading of the orbit monitor next to this quadrupole would represent the offset of the magnetic center to the electric center of the pickup. Such values obtained pickup by pickup represent a beam based calibration of the pickups. In order to determine the passage of the beam through the center of a particular quadrupole its strength is modulated sinusoidially by about 10^{-4} of its actual strength at a frequency around 10 Hz. With a sensitive oscillation detector somewhere in the ring the beam oscillation at the strength modulation frequency is measured. Steering the beam through the quadrupole one finds a position for which the modulation signal disappears. In that case the beam passes through the center of the modulated quadrupole. In practice this procedure has been used in LEP for many orbit pickups and the offsets have been measured with a precision of about 80 μm. More details can be found in [8].

3.3 Longitudinal Spectra

In most machines monitors for longitudinal beam oscillations are available. These monitors are used to measure the synchrotron tune as the maximum of the amplitude response spectrum. By going one step further and fitting a theoretical curve to the whole amplitude spectrum also the longitudinal

damping time, a quantity that otherwise is difficult to measure, can be obtained. Figure 13 which has been provided by [9] shows a nice measurement example.

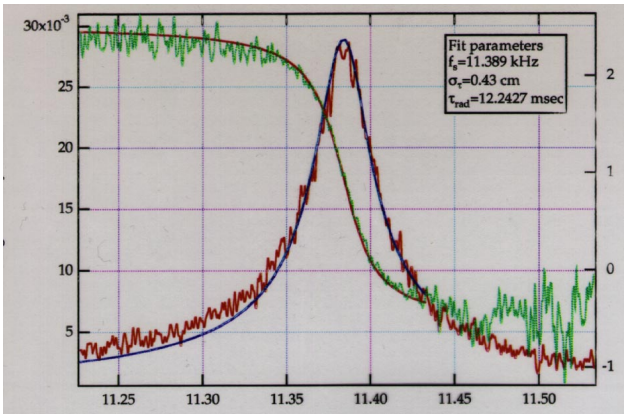

Figure 13: Measurement of the longitudinal damping time from a fit to the longitudinal beam spectrum

3.4 Proton loss rates minimized at HERA

As in most proton machines the requirements for the stability of the betatron tunes is also very tight for the HERA proton ring. Tune modulations of the order of 10^{-5} to 10^{-4} were measured and attributed to the following main sources: power supply ripples, earth motion, chromaticty and the beam-beam interaction. At these levels tune modulation cause particle losses via diffusion and hence one would like to stabilize the tunes as much as possible. As the power supply ripple at 300 Hz and 600 Hz is the dominant modulation source the following compensation scheme was tried. A single quadrupole in the ring was excited with a separated power supply at 300 Hz and 600 Hz respectively. The strength and the phase of the excitation was variied in order to find a minimum in the measured proton loss rate. Figure 14 shows the effect on the beam for the case of the optimum compensation settings. More details can be found in [10].

4 EXPLOITATION OF DSP TECHNIQUES

This subject has been treated in detail during the oral presentation, but for the writeup on five pages priority has been given to the previous two chapters. But a complete writeup of this chapter can be found in [11]

5 CONCLUSIONS

Beam instrumentation is a key element in accelerator operation and machine studies. In some cases the instruments are very sophisticated detectors demanding many manyears of development. Very nice and important observations can be made by clever use of conventional instruments. The exploitation of digital signal treatment adds a powerful component to beam instrumentation.

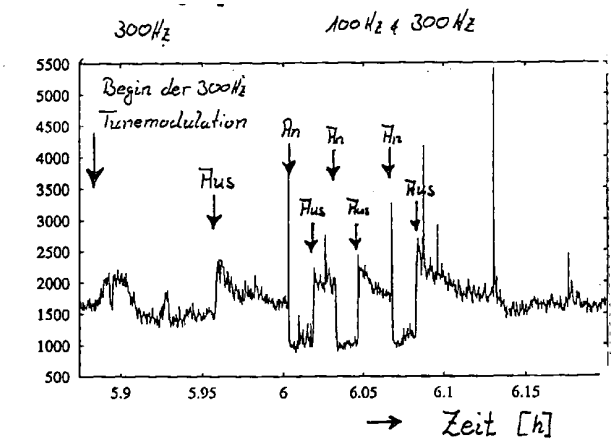

Figure 14: Measured proton loss rate as a function of time during a period when the tunemodulation was compensated (”AN”) or was not compensated (”AUS”).

6 REFERENCES

[1] T. Shintake et al., **First Beam Test of Nanometer Spot Size Monitor Using Laser Interferometry**, Contributed to the 19th Accelerator Meeting in Japon, JAERI, Tokai, Ibaraki, Japan, July 20-22, 1994, KEK Preprint 94-129, and references therein.

[2] J. Buon et al., Nucl. Instrum. Meth. A306 (1991) 93-111 and P. Puzo, PhD thesis, Orsay University (1994)

[3] E. Rossa et al., Proc. of EPAC 1990, Nice, Edition Frontières, Gif-sur-Yvette, 1990, pp 768-770.

[4] J. Whitaker, University of Michigan, mentioned by: G. Mourou, Invited talk at the workshop: *Les quatriemes journées de caractérisation microonde et materiaux*, April 4th 1996, Chambery France.

[5] P. Kung et al., **Generation and Measurement of 50 fs(rms) Electron Pulses**, SLAC-PUB-6507, June 1994, submitted to Physical Review Letters.

[6] H. Schmickler, **Measurement of the Central Frequency of LEP**, Lep-MD Note 89, 23 July 1993.

[7] L. Arnaudon et al., **Effecets of Terrestial Tides on the LEP Beam Energy**, NIM A 357 (1995), pp 249-252.

[8] I. Barnett et al., **Dynamic Beam Based Calibration of Orbit Monitors at LEP**, Proc. of the 4th International Workshop on Accelerator Alignment (IWAA 95), KEK Proc. 95-12, also CERN SL/95-97(BI).

[9] J. M. Byrd, jmbyrd@lbl.gov, Private Communication

[10] O. Brüning, **Tunemodulation in HERA-P**, HERA Seminar Bad Lauterberg, Feb. 2-7 1995, DESY-HERA 95-03

[11] H. Schmickler, **Digital Signal Processing**, Proceedings of the first Diagnostics and Instrumentation Workshop (DIPAC), Montreux May 3-5 1993, CERN SL/93-35 (BI)